Investigating Interacting Fermionic Models with Locality-Preserving Qubit Encodings

Ashutosh Tripathi

Department of Theoretical Physics, TIFR, Mumbai

Frontiers of Quantum Computing and Classical Tensor Networks for Gauge Theories
Kyoto, 16-20, November 2026

Based on arXiv:2609.16142

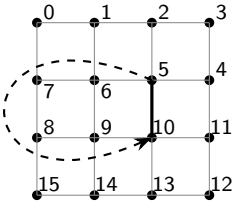
Outline

1. **Motivation and model**
   Local fermions and the cost of qubit encodings
2. **Derby–Klassen mapping**
   Local operators, constraints, and Clifford preparation
3. **Variational simulations and numerical results**
   HVA/VQD, spectra, observables, and DK–JW comparisons
4. **Conclusion and outlook**

Derby, Klassen, Bausch and Cubitt, *Phys. Rev. B* **104**, 035118 (2021).

The problem: local fermions, nonlocal qubit operators

- Strongly correlated lattice fermions are naturally expressed using local hopping and interactions.
- Fermionic anticommutation must be represented on qubits.
- In two dimensions, a conventional Jordan–Wigner (JW) ordering produces long parity strings.
- **Question:** can we preserve geometric locality while retaining the correct fermionic Hilbert space?



Jordan and Wigner, *Z. Phys.* **47**, 631 (1928).

Qubit encoding

Qubit-based computation

- Map fermions to qubits (JW, DK).
- Use standard circuits and readout.
- Trade-off: parity strings versus auxiliary qubits and constraints.

Native fermionic processors

- Exchange statistics are native.
- Trade-off: Coherent gates, control, readout and error correction remain challenges.

Our focus: Investigate locality-preserving encoding for conventional qubit-based circuits.

González-Cuadra *et al.*, *PNAS* **120**, e2304294120 (2023).

Interacting spinless fermions

$$H_F = -t \sum_{\langle ij \rangle} (a_i^\dagger a_j + a_j^\dagger a_i) - \mu \sum_i (n_i - \tfrac{1}{2}) + V \sum_{\langle ij \rangle} (n_i - \tfrac{1}{2})(n_j - \tfrac{1}{2}), \qquad t = 1.$$

- Nearest-neighbor hopping competes with density–density repulsion.
- At $\mu = 0$, particle–hole symmetry is especially useful for low-energy benchmarks.
- We compare encoded VQE/VQD with exact diagonalization (QuSpin).
- Two targets: **accurate physical observables** and **reduced logical-circuit resources**.

VQE: Peruzzo *et al.*, *Nat. Commun.* **5**, 4213 (2014); VQD: Higgott *et al.*, *Quantum* **3**, 156 (2019),

QuSpin: Weinberg and Bukov, *SciPost Phys.* **7**, 020 (2019).

Fermionic vertex and edge operators

Start from Majorana operators associated with each fermionic mode:

$$\gamma_i = a_i^\dagger + a_i, \qquad \bar{\gamma}_i = i(a_i^\dagger - a_i).$$

Vertex operator

$$V_i = i\bar{\gamma}_i\gamma_i = 1 - 2n_i$$

Local occupation / fermion parity at site i.

Edge operator

$$E_{ij} = -i\gamma_i\gamma_j = -E_{ji}$$

Oriented edge encoding fermionic exchange signs.

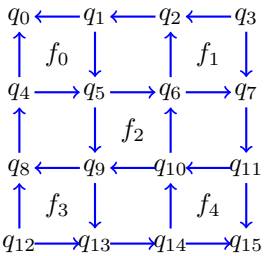
Key algebraic relations

$$V_i^2 = E_{ij}^2 = I, \qquad [V_i, V_j] = 0,$$
$$\{V_i, E_{ij}\} = \{V_j, E_{ij}\} = 0, \qquad \{E_{ij}, E_{jk}\} = 0 \quad (i, j, k \text{ distinct}).$$

Derby, Klassen, Bausch and Cubitt, *Phys. Rev. B* **104**, 035118 (2021).

Auxiliary face qubits preserve locality

- **Vertex qubits** represent fermionic modes (q).
- **Auxiliary face qubits** occupy alternating plaquettes (f).
- Face qubits allow nearest-neighbor hopping to have **bounded Pauli support**.



Arrows indicate the chosen edge orientation; stabilizer constraints select $\mathcal{H}_{\text{phys}} \subset \mathcal{H}_{\mathcal{Q}}$.

Qubit representation of vertex and edge operators

Vertex (occupation)

$$\widetilde{V}_j = Z_j, \qquad \widetilde{n}_j = \frac{I - Z_j}{2}$$

Oriented edge $j \to k$

$$\widetilde{E}_{jk} = X_j Y_k P_{jk}, \quad \widetilde{E}_{kj} = -\widetilde{E}_{jk}$$

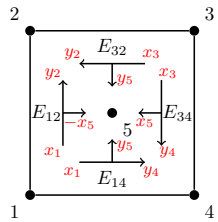
Face-qubit factors :

$$\widetilde{E}_{jk} = \begin{cases} X_j Y_k X_{F(j,k)}, & \text{downward edge,} \\ -X_j Y_k X_{F(j,k)}, & \text{upward edge,} \\ X_j Y_k Y_{F(j,k)}, & \text{horizontal edge.} \end{cases}$$

- $F(j,k)$ denotes the auxiliary face qubit associated with the edge.
- If an outer edge has no face qubit, its face Pauli factor is omitted.

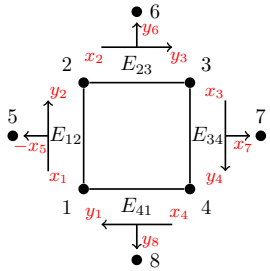
Odd and even loops: physical constraints

Odd face: identity



$$\prod_{(ij)\in\partial f} i\widetilde{E}_{ij} = I$$

Even face: stabilizer



$$S_f = Z_1 Z_2 Z_3 Z_4 \, X_5 Y_6 X_7 Y_8$$

Odd loops impose no new condition; **even loops require** $S_f|\psi_{\text{phys}}\rangle = |\psi_{\text{phys}}\rangle$.

Structural analogy to Gauss-law constraints

DK encoding

$(I - S_f)|\psi\rangle = 0$

Constraint selects a physical code space inside an enlarged Hilbert space.

Hamiltonian lattice gauge theory

$G_x|\psi\rangle = 0$

Gauss law selects gauge-invariant physical states.

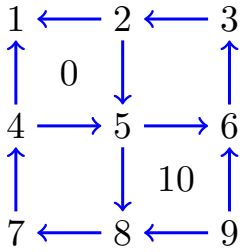
- In both settings, physical states are identified by constraints.
- A penalty can suppress violations: $\widetilde{H} \to \widetilde{H} + \frac{\lambda}{2}\sum_f (I - S_f)$.
- **Distinction:** DK stabilizers implement an encoding; they do not introduce a dynamical gauge field.

The encoded Hamiltonian remains geometrically local

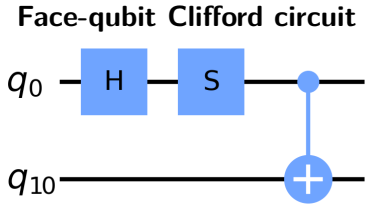
$$\widetilde{H}_F = -\frac{t}{2}\sum_{\langle ij\rangle}\eta_{ij}(X_iX_j + Y_iY_j)P_{ij} + \frac{\mu}{2}\sum_i Z_i + \frac{V}{4}\sum_{\langle ij\rangle} Z_iZ_j.$$

- P_{ij} is a Pauli acting on a nearby auxiliary face qubit, where applicable.
- The lattice interaction remains a bounded-support Pauli operator.
- The ansatz generators commute with the stabilizers: $[U(\boldsymbol{\theta}), S_f] = 0$.
- Starting in $\mathcal{H}_{\text{phys}}$ keeps the evolution in $\mathcal{H}_{\text{phys}}$.

Physical-sector preparation: 3×3 lattice and Clifford circuit



Vertices $q_1, \ldots, q_9$; faces q_0, q_{10}



q_0, q_{10} are the two face-qubit wires

$$S_1 = X_0 Y_{10}\, Z_2 Z_3 Z_5 Z_6, \qquad S_2 = Y_0 X_{10}\, Z_4 Z_5 Z_7 Z_8,$$
$$S_1' = Z_0 Z_{10} Z_2 Z_3 Z_5 Z_6, \qquad S_2' = Z_0 Z_4 Z_5 Z_7 Z_8.$$

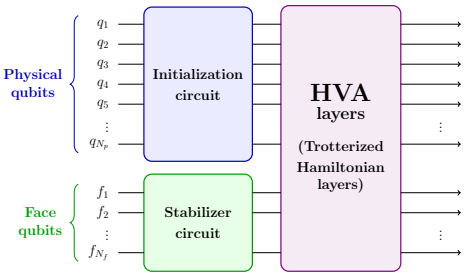
$S_1|\psi_{\text{phys}}\rangle = S_2|\psi_{\text{phys}}\rangle = |\psi_{\text{phys}}\rangle$. Primes denote the diagonalized stabilizers.

Hamiltonian variational ansatz (HVA)

$$|\psi(\boldsymbol{\theta})\rangle = \prod_{\ell=1}^{N_l} \prod_{\alpha} e^{-i\theta_{\ell\alpha}\widetilde{H}_\alpha} |\psi_{\text{phys}}^{(0)}\rangle.$$

- Variational gates built from hopping and interaction operators.
- Compact local gates avoid extended JW parity strings.
- Conserved particle number lets us initialize and optimize in specific sectors.

DK-HVA circuit structure



Clifford preparation sets the physical sector.

Wecker, Hastings and Troyer, *Phys. Rev. A* **92**, 042303 (2015).

Local hopping: DK encoding and circuit structure

$$h_{ij} = -t(a_i^\dagger a_j + a_j^\dagger a_i)$$

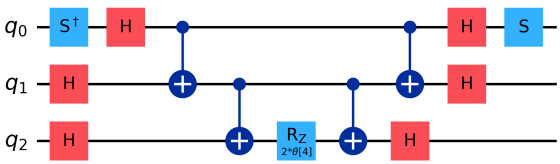
Jordan–Wigner:

$$\widetilde{h}_{ij}^{\mathrm{JW}} = -\frac{t}{2}\left(X_i Z_{(i,j)} X_j + Y_i Z_{(i,j)} Y_j\right)$$

Derby–Klassen:

$$\widetilde{h}_{ij}^{\mathrm{DK}} = -\frac{t\eta_{ij}}{2}\left(X_i X_j + Y_i Y_j\right) P_{ij}$$

$$P_{ij} = \begin{cases} Y_{F(i,j)} & \text{horizontal edge,} \\ X_{F(i,j)} & \text{vertical edge,} \\ I & \text{no adjacent face qubit.} \end{cases}$$

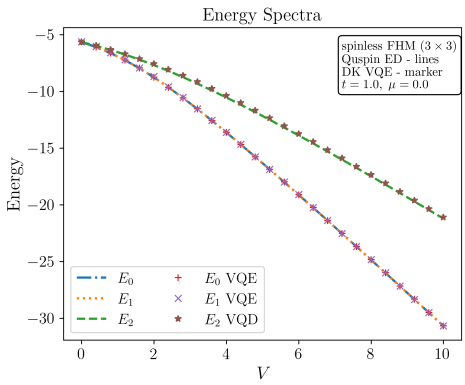


$Z_{(i,j)} = \prod_{k \text{ between } i,j} Z_k$ in JW order; $\eta_{ij} = \pm 1$ depends on the oriented DK edge.

The 3×3 low-energy spectrum: sector-resolved VQE/VQD

Numerical setup: noiseless statevector VQE/VQD, exact expectation values; ED reference.

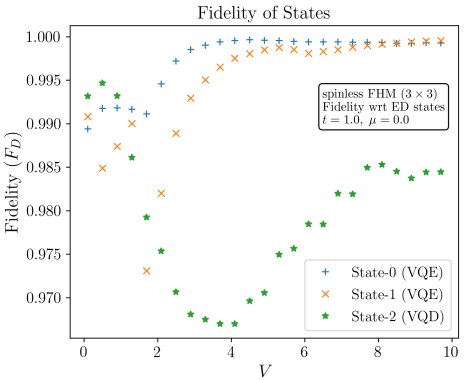
- At $\mu = 0$, four- and five-particle sectors have degenerate ground states.
- VQE independently targets each particle-number sector.
- Within-sector VQD obtains higher states.
- Compare three lowest energies with ED.



Fidelity with exact diagonalization: 3×3

$$F_n = \left| \left\langle \psi_n^{\mathrm{ED}} \middle| \psi_n^{\mathrm{VQE/VQD}} \right\rangle \right|^2 .$$

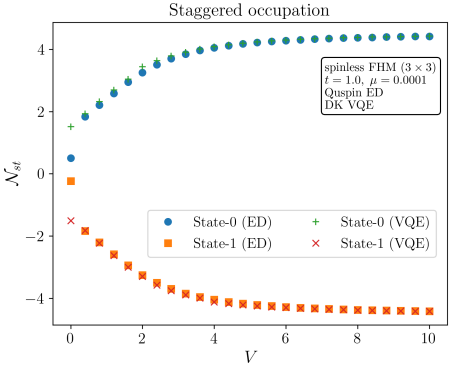
- Particle-number conservation ensures orthogonality between the two states.
- Fidelity remains close to unity, with reduced accuracy at intermediate V, particularly for the VQD state.

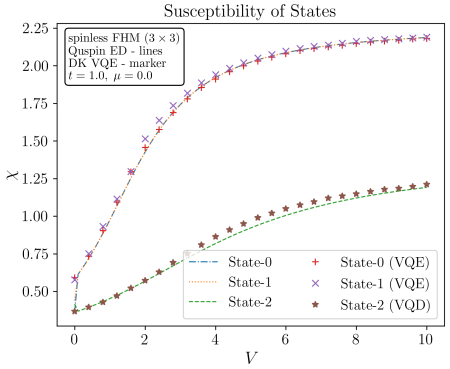


Observables: staggered occupation and susceptibility

$$\mathcal{N}_{\text{st}} = \sum_{(x,y)} (-1)^{x+y} \left(n_{x,y} - \tfrac{1}{2}\right)$$

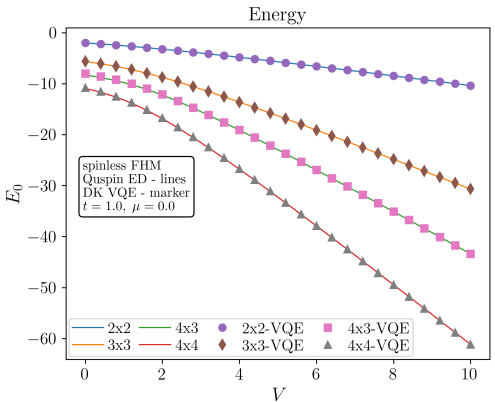
$$\chi = \frac{\langle \mathcal{N}_{\text{st}}^2 \rangle}{L_x L_y}$$





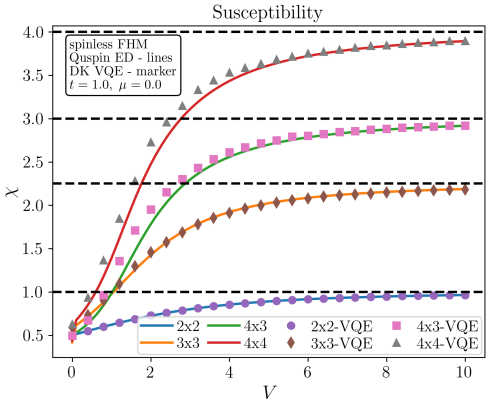
Different lattice sizes: ground-state energies

- 2×2, 3×3, 4×3, 4×4 benchmarks.
- DK-HVA energies compared with QuSpin ED.
- Agreement remains good over the reported interaction range.



Different lattice sizes: susceptibility

- Susceptibility probes ordering correlations, not just energy.
- Agreement weakens at intermediate V for some sizes.
- At strong repulsion, approaches $\chi \simeq (L_x L_y)/4$ for half-filling ordering.



Finite chemical potential: compare DK and JW

Individual eigenvectors can be ambiguous within a degenerate subspace. F_D tests overlap with the physically relevant eigenspace.

$$F_D = \sum_{a \in D} |\langle \phi_a | \psi \rangle|^2.$$

$V = 2$, $\mu = 0.5$, eight variational layers; noiseless classical simulation.

3×3, **ED** $E_0 = -9.01941$

Ansatz	VQE E_0	Fidelity	Time (min)
JW-HVA	-8.9262	.9808	38.4
DK-HVA	-8.9219	.9798	2.3

4×4, **ED** $E_0 = -16.8769$

Ansatz	VQE E_0	F_D	Time (min)
JW-HVA	-16.4095	.9000	202.0
DK-HVA	-16.4165	.9011	12.0

- Reported *classical optimization times* are implementation-dependent, not hardware speedups.
- 4×4 fidelity is summed over two nearly degenerate low-energy states.

Logical resources: where locality helps

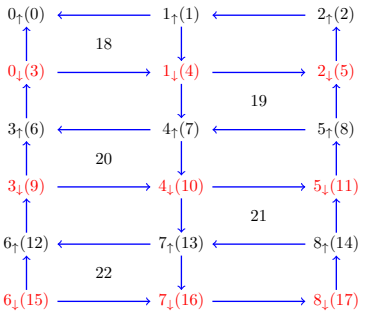
Let $L = L_x L_y$ and N_l be the number of HVA layers.

	CNOT count	CNOT depth
DK-HVA	$10N_l(2L - L_x - L_y) + N_S$	$24N_l$
JW-HVA	$N_l(2L_x + 4)(2L - L_x - L_y)$	$(24 + L_x)N_l$

- Same number of HVA variational parameters in the two mappings.
- DK adds N_S fixed stabilizer-preparation CNOTs and auxiliary qubits.
- These are **logical** resource estimates for open boundaries, not hardware-transpiled gate counts.
- Fermionic SWAP networks can substantially improve naive JW routing.

Fermionic SWAP networks: Kivlichan *et al.*, *Phys. Rev. Lett.* **120**, 110501 (2018).

Spinful extension: encoding same-spin hopping locally



- $\uparrow$ and $\downarrow$ occupy adjacent vertex sites.
- Same-spin hopping is between next-nearest encoded vertices i, j.
- Use an intermediate vertex k and two local edges:

$$iE_{ij} = (iE_{ik})(iE_{kj}).$$

$$a_i^\dagger a_j + a_j^\dagger a_i \longmapsto \frac{\eta_{ik}\eta_{kj}}{2}(X_i Z_k X_j + Y_i Z_k Y_j) P_{ik} P_{kj}$$

P_{ik}, P_{kj} act on nearby face qubits when present.

Conclusion and Outlook

1. **Local encoding:** DK uses auxiliary face qubits to represent local fermionic terms by compact Pauli operators.
2. **Physical sector:** Clifford preparation plus stabilizer-preserving HVA implements the fermionic constraints without requiring a variational penalty.
3. **Physical benchmarks:** energies, subspace fidelities, staggered occupation and susceptibility agree well with ED for the finite lattices studied.
4. **Resources and outlook:** logical-circuit savings relative to studied JW-HVA schemes trade against auxiliary qubits; spinful benchmarking and comparisons with fermionic tensor networks remain open.

Thank you!

Questions?

Collaborators:

Debasish Banerjee

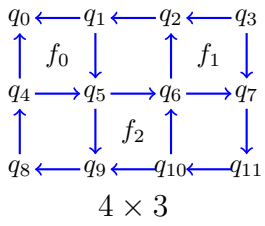
Sandip Maiti

Nilmani Mathur

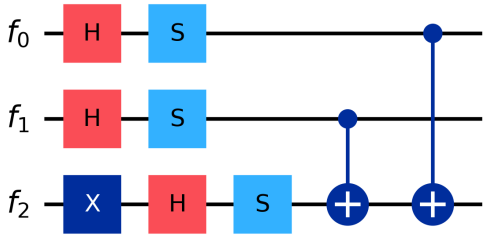


arXiv:2609.16142

Backup: 4×3 lattice and diagonalizing Clifford gates



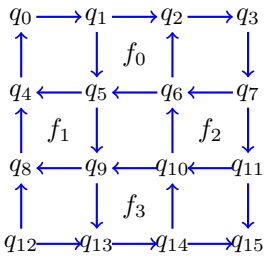
Schematic: 12 vertex qubits and 3 auxiliary face qubits.



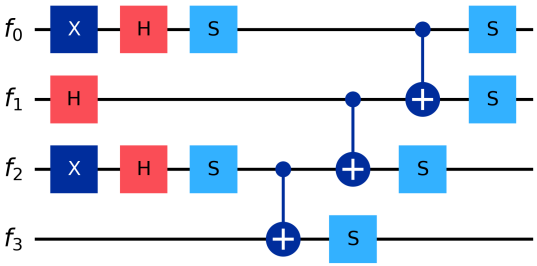
Face-register Clifford gates H, S, X and CNOT.

$S_f|\psi_{\text{phys}}\rangle = |\psi_{\text{phys}}\rangle$ for each independent even-face stabilizer.

Backup: 4×4 lattice and diagonalizing Clifford gates



Schematic: 16 vertex qubits and 4 auxiliary face qubits.



Face-register Clifford gates X, H, S and CNOT.

The fixed Clifford network diagonalizes the independent loop stabilizers.

Backup: VQD within a fixed particle-number sector

$$\mathcal{C}_{N_p}(\boldsymbol{\theta}) = \langle\psi_{N_p}(\boldsymbol{\theta})|H|\psi_{N_p}(\boldsymbol{\theta})\rangle + \alpha|\langle\phi^{(0)}_{N_p}|\psi_{N_p}(\boldsymbol{\theta})\rangle|^2.$$

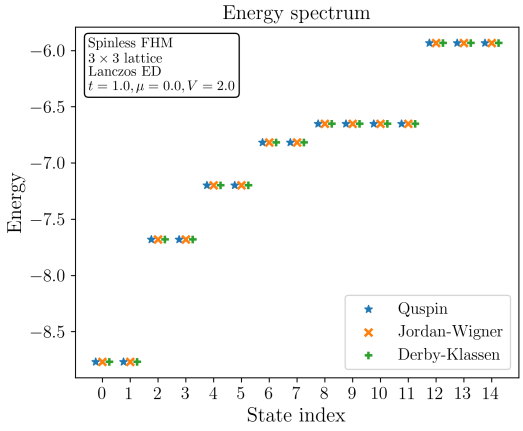
- For the 3×3 benchmark $\alpha = 20$.
- Deflation must compare states in the *same* particle-number sector.
- Ground states in distinct sectors are orthogonal automatically.

Backup: explicit resource comparison with EfficientSU2

Ansatz	Parameters	CNOT gates
SU2-full	$2(N_l+1)L_xL_y$	$2N_lL_xL_y(L_xL_y-1)$
SU2-linear	$2(N_l+1)L_xL_y$	$N_l(L_xL_y-1)$
DK-HVA	$N_l(2L_xL_y-L_x-L_y+1)$	$10N_l(2L_xL_y-L_x-L_y)+N_S$
JW-HVA	$N_l(2L_xL_y-L_x-L_y+1)$	$N_l(2L_x+4)(2L_xL_y-L_x-L_y)$

Logical upper bounds for open boundary conditions, as tabulated in the paper.

Backup: encoded fermion spectra

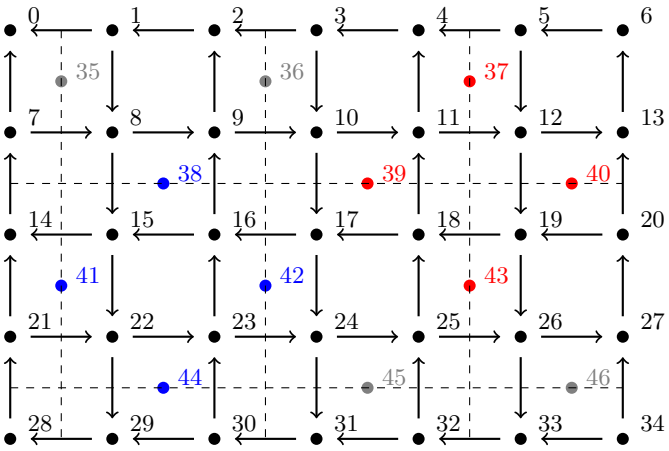


Limitations and directions for ongoing work

Route	Current bottleneck	Active direction
Native fermions	Gate control, loss/errors, parity-compatible operations	Programmable fermion registers, hybrid gates and error correction
Fermionic TN	2D contraction and increasing bond dimension	Improved fPEPS contractions, symmetries and optimization
Qubit encoding (DK)	Extra face qubits, state preparation, routing and noise	Resource-aware encoding, symmetry verification; spinful benchmarks

Outlook: extend the encoded benchmarks beyond the spinless model, and compare against fermionic tensor networks where controlled reference data are available.

7×6 lattice



Backup: foundational references

- Jordan and Wigner, *Z. Phys.* **47**, 631 (1928) — fermion–spin transformation.
- Peruzzo *et al.*, *Nat. Commun.* **5**, 4213 (2014) — VQE.
- Wecker, Hastings and Troyer, *Phys. Rev. A* **92**, 042303 (2015) — Hamiltonian variational ansatz.
- Higgott, Wang and Brierley, *Quantum* **3**, 156 (2019) — VQD.
- Derby, Klassen, Bausch and Cubitt, *Phys. Rev. B* **104**, 035118 (2021) — compact mapping.